



CHORUS

This is the accepted manuscript made available via CHORUS. The article has been published as:

Attosecond measurement via high-order harmonic generation in low-frequency fields

Graham G. Brown, Dong Hyuk Ko, Chunmei Zhang, and P. B. Corkum

Phys. Rev. A **105**, 023520 — Published 24 February 2022

DOI: [10.1103/PhysRevA.105.023520](https://doi.org/10.1103/PhysRevA.105.023520)

Attosecond Measurement via High-Harmonic Generation in Low-Frequency Fields

Graham G. Brown,* Dong Hyuk Ko, Chunmei Zhang, and P. B. Corkum

Department of Physics, University of Ottawa, Ottawa, Canada K1N 6N5 and

National Research Council of Canada, Ottawa, Canada K1A 0R6

(Dated: November 3, 2021)

The spectral phase of high harmonic and attosecond pulses is typically shaped by the interaction of the recollision electron with the strong field in the continuum. However, the phase of the transition moment coupling bound and continuum states can be significant in shaping the emitted radiation. It has been commonly assumed that the propagation and recombination steps of the recollision process can be described independently. Here, we investigate the effect that the transition moment has on recollision trajectories by incorporating the transition moment phase into the Lewenstein model of recollision. We then use our model to investigate the all-optical measurement of the transition moment phase around the Cooper minimum in argon and the spectral minimum due to two-centre interference in a diatomic molecular system. Our results indicate that, while all-optical methods are generally sensitive to the transition moment phase, they are insensitive to the phase shifts due to two-centre interference and ionic structure. Thus, we have resolved the apparent discrepancy between studies with conflicting conclusions regarding the sensitivity of all-optical approaches to the transition moment phase. Our work demonstrates that all-optical measurements focus on photo-recombination time delays attributable to electronic structure and dynamics. Our method will allow any laboratory capable of generating attosecond pulses to perform these measurements, even at wavelengths where the single photoionization cross-section becomes small.

Visible or infrared ultrafast optical technology requires a nonlinear interaction for generating ultrashort pulses and for measuring ultrafast phenomena. Nonlinearity is essential because it allows information to be shared between the frequencies that make up any wave packet. In a laser oscillator, nonlinear optics ensures that there is an exchange of energy between modes that allows them to become locked in phase. For a measurement, nonlinearity is equally important and the nonlinear process can, but does not need to be, all-optical. The issue that we address in this paper is, “are all-optical approaches [1, 2] permitted in attosecond science”?

A semi-classical theory of extreme nonlinear optics and recollision was introduced in this journal in 1994 [3]. This theory, known as the Lewenstein model, provided the classical model [4] of recollision with a rigorous quantum mechanical foundation. Within this theory, the three-step recollision process consists of an electron in the presence of a strong field (1) tunnelling into the continuum, (2) being accelerated by the strong field, and (3) recombining into its initial state and emitting an XUV photon. The phase of the emitted radiation is predominantly shaped by the continuum propagation of the ionized electron [5, 6], but can be significantly shaped by the phase of the transition moment coupling the initial and continuum states [7–10].

At that time, the important issue was high-harmonic generation and so the potential of using extreme nonlinear optics for measurement was not addressed. Yet the formalism introduced in that paper clarifies what has since become a very controversial issue of measurement [8, 10], just as it clarified the issue of attosecond pulse

generation at the time it was published: whether all-optical approaches are permitted in attosecond science is directly related to how each step of the recollision process is related.

The controversy can be understood by considering the three-step model of high-harmonic generation, introduced in 1993 [4]. Although not stated at the time, the three steps appear independent [11]. Quantitative rescattering [12] (introduced later) made the independence of the steps a formal assumption. If the steps are truly independent, then nonlinear optics can only measure those steps that are optically influenced and it is the recollision electron trajectory in the continuum that is most easily influenced. Thus, it would seem that nonlinear optics might have little to say about the dynamics of ionization or recombination. This perspective is supported by studies comparing all-optical measurement with photoionization-based attosecond measurement [13] in systems exhibiting a transition moment phase shift due to two-centre interference [8] and a shape resonance [10]. However, this perspective is challenged by recent experimental and theoretical work demonstrating the all-optical measurement of the transition moment phase around the Cooper minimum in argon [14].

It is not that attosecond dynamics cannot be measured by other nonlinearities. There is little controversy, but much complexity, about attosecond measurements using photoelectron spectroscopy [2, 13, 15]. This, however, is not merely an academic issue. High harmonics seem to be a universal response of matter when irradiated by an intense field [16, 17] and it is important to make attosecond measurements in all these media. If we are confined to photoelectron spectroscopy, attosecond measurements will only be possible in near vacuum.

However, one can easily understand an alternate per-

* graham.brown@uottawa.ca

spective. The observation of coherent radiation from recollision requires the recolliding electron to return to its initial state [3]. The requirement for recombination to the same initial state acts analogously to phase-matching in determining attosecond pulse emission. If the transition moment coupling the initial and continuum states is complex, then phase-matching favours components of the continuum electron wave packet appropriately phased with respect to both the initial state and the transition moment to dominate dipole emission. That is, the transition moment not only affects ionization and recombination, but continuum propagation as well.

In this letter, we will show how this occurs during recollision and, thereby, how fully optical measurements of attosecond dynamics can be accomplished. We do this by first extending the Lewenstein model of recollision, the strong-field approximation (SFA) [3], to account for phase shifts in the transition moment between bound and continuum states. We then describe all-optical attosecond measurement [1] and investigate its application in systems with transition moment phase shifts due to electronic structure [18] and due to ionic structure [8, 19]. Our results show that the sensitivity of all-optical measurement to the transition moment phase shift depends on the origin of the phase shift. In particular, we show all-optical measurement is insensitive to phase shifts arising from ionic structure, but sensitive to phase shifts pertaining to electronic structure and dynamics.

I. THE STRONG FIELD APPROXIMATION AND ATTOSECOND *IN SITU* MEASUREMENT

A. The Strong Field Approximation with a Transition Moment Phase

We begin with a single-active electron atom with ground state $|\psi_0\rangle$ and ionization potential I_p . We then consider recollision driven by a time-dependent strong laser field $E(t)$ polarized along \hat{z} with vector potential $A(t)$. We omit vector notation because all parameters herein are oriented along \hat{z} . We define $P(t) = k + A(t)$ as the recollision electron kinetic momentum, where k is the electron canonical momentum. We work within the same assumptions as in [3]: (i) the contribution of all bound states except the ground state can be neglected, (ii) ground state depletion is neglected, and (iii) the influence of the ionic potential in the continuum is neglected.

Within the SFA, the time-dependent recollision dipole spectrum at time t_r can be expressed as follows [3]:

$$D(t_r) = -i \int dk \int_{-\infty}^{t_r} dt_b d^*(P(t_r)) \times e^{-i[S(k, t_b, t_r) + I_p(t_r - t_b)]} E(t_b) d(P(t_b)), \quad (1)$$

where t_b is the time of ionization, t_r is the time of recombination, $S(k, t_b, t_r)$ is the semi-classical action,

$$S(k, t_b, t_r) = \frac{1}{2} \int_{t_b}^{t_r} [k + A(\tau)]^2 d\tau, \quad (2)$$

and $d(k)$ is the complex transition moment along \hat{z} ,

$$d(k) = \langle k | \hat{z} | \psi_0 \rangle. \quad (3)$$

The total integrand phase is then

$$\Phi_{tot}(k, t_b, t_r) = S(k, t_b, t_r) + I_p(t_r - t_b) + \Phi(k + A(t_b)) - \Phi(k + A(t_r)), \quad (4)$$

where $I_p(t_r - t_b)$ describes the evolution of the ground state wavefunction and $\Phi(k) = \arg(d(k))$.

Eq. (1) is typically solved using a saddle-point approximation [20], wherein the stationary points (i.e. the saddle-point solutions) of the integrand phase in Eq. (4) are used to select the dominant components of the integrand. The integral is then approximated as a weighted summation over the integrand evaluated at the saddle-point solutions. Thus, the stationary-phase analysis is analogous to phase-matching, selecting only components of the recollision electron wave packet which are appropriately phased [3].

Within the initial description of the SFA, it is assumed that the integrand phase is predominantly determined by the semi-classical action and the evolution of the ground state. That is, it is assumed that the transition moment varies slowly and can be neglected in the saddle-point analysis. This approximation is applicable in many systems and the saddle-point solutions provide the link between the quantum mechanical and semi-classical recollision models [4].

As implied in [3], however, this assumption does not apply to systems with a rapidly varying transition moment. In such systems, the variation of the transition moment phase can be on the same order as the semi-classical action and it must be included in the saddle-point analysis. The measurement of the effect that this phase has on the saddle-point solutions is the subject of this letter.

B. Attosecond *In Situ* Measurement

Optical measurements of recollision are accomplished by perturbing recollision with a weak infrared field. The perturbation modulates recollision trajectories and these modulations are used to reconstruct recollision dynamics [2]. Since these measurements are performed during the recollision process itself, they are referred to as *in situ* measurement.

Many variations of *in situ* measurement exist [1, 2, 21, 22]. We consider a measurement used to characterize high-harmonic spectra generated with long driving

pulses wherein a co-polarized, co-phased, and collinear weak second harmonic of the driving field perturbs recollision [1]. The driving and perturbing field vector potentials at time t are given, respectively, as follows:

$$A(t) = A_0 \sin(\omega_0 t), \quad (5)$$

$$A_p(t) = \eta A_0 \sin(2\omega_0 t + \phi), \quad (6)$$

where A_0 is the driving field vector potential amplitude, ω_0 is the driving field frequency, and η and ϕ are the relative amplitude and phase between the driving and perturbing fields. It is assumed that $\eta \ll 1$ and is sufficiently small such that the perturbing field does not affect the saddle-point analysis.

In situ measurement was originally described in systems wherein the transition moment phase is slowly varying. Thus, the effect of the perturbing field is included solely within Eq. (2) and the effect of the perturbing field on the transition moment is neglected. With this assumption, the phase shift of the recollision electron induced by perturbation results from the expansion of the semi-classical action to first-order in η :

$$\sigma_0(k, t_b, t_r, \phi) = \int_{t_b}^{t_r} [k + A(\tau)] A_p(\tau, \phi) d\tau. \quad (7)$$

Here, however, we are interested in the case where the transition moment phase is rapidly varying and cannot be neglected. In this case, the total perturbation-induced phase shift is found by expanding the total phase in Eq. (4) to first-order in η and is given as follows:

$$\sigma(k, t_b, t_r, \phi) = \sigma_0(k, t_b, t_r, \phi) + A_p(t_b, \phi) \Phi'(P(t_b)) - A_p(t_r) \Phi'(P(t_r)). \quad (8)$$

This phase shift is affected by the transition moment in two ways. First, the transition moment affects the saddle-point solutions and, thus, directly affects the semi-classical action, $\sigma_0(k, t_b, t_r, \phi)$. Second, the measurement is affected by the influence of the perturbing field on the transition moment.

With Eqs. (5-8), the perturbation-induced phase shift can be factored into rapidly and slowly varying components, $\Sigma(k, t_b, t_r)$ and $\cos(\phi - \theta(k, t_b, t_r))$, respectively, as follows [1]:

$$\begin{aligned} \sigma(k, t_b, t_r, \phi) &= \sigma_c(k, t_b, t_r) \sin(\phi) + \sigma_s(k, t_b, t_r) \cos(\phi) \\ &= \Sigma(k, t_b, t_r) \cos(\phi - \theta(k, t_b, t_r)), \end{aligned} \quad (9)$$

where

$$\Sigma(k, t_b, t_r) = \sqrt{\sigma_c^2(k, t_b, t_r) + \sigma_s^2(k, t_b, t_r)}, \quad (10)$$

$$\theta(k, t_b, t_r) = \arctan\left(\frac{\sigma_c(k, t_b, t_r)}{\sigma_s(k, t_b, t_r)}\right). \quad (11)$$

We now consider the perturbed dipole emission from two adjacent half-cycles, $D_L(t)$ and $D_R(t)$, of the driving field, which we label as left (L) and right (R), respectively. Symmetry requires that the unperturbed dipole emission from the left and right half-cycles exhibit a π -phase difference and that the perturbation-induced phase shift in each half-cycle is equal but opposite in sign. With this, the superposition of the dipole emission from the left and right half-cycles, $D(t_r, \phi)$, satisfies the following:

$$D(t_r, \phi) \propto \int dk \int_{-\infty}^{t_r} dt_b \sigma(k, t_b, t_r, \phi) D_L(k, t_b, t_r). \quad (12)$$

The dipole spectrum at even harmonic $2N$ (integer N) is found through the Fourier transform of Eq. (12) at frequency $2N\omega_0$. We define $\Phi_{tot}(t) = -i \ln(\Sigma(k, t_b, t_r) + D_L(t))$, such that

$$\begin{aligned} \tilde{D}(2N\omega_0, \phi) &\propto \int dk \int_{-\infty}^{\infty} dt_r \int_{-\infty}^{t_r} e^{i\Phi_{tot}(t_r)} \\ &\quad \cos(\phi - \theta(k, t_b, t_r)) e^{2iN\omega_0 t_r}. \end{aligned} \quad (13)$$

After finding the unperturbed saddle-point solutions, the variation of the $2N^{\text{th}}$ even-harmonic intensity with respect to the relative phase ϕ is given as

$$\left| \tilde{D}(2N\omega_0, \phi) \right|^2 \propto \cos^2(\phi - \theta(k, t_b, t_r)). \quad (14)$$

Experimentally, the relative phase which maximizes the even-harmonic signal is recorded while varying the relative phase between the driving and perturbing fields. From Eq. (14), the even-harmonic signal is maximized when $\phi = \theta(k, t_b, t_r)$. Thus, we call $\theta(k, t_b, t_r)$ the maximizing phase. Since the maximizing phase has an analytic expression, the measured maximizing phase can be related directly to the recollision dynamics for each even harmonic. Thus, the feasibility of *in situ* measurement to measure the transition moment phase in the subsequent section will be determined through the maximizing phase $\theta(k, t_b, t_r)$.

II. *IN SITU* MEASUREMENT AND THE TRANSITION MOMENT PHASE

We are now ready to describe *in situ* measurement in systems exhibiting a transition moment phase shift. We first consider the case of a transition moment phase shift due to electronic structure, using the Cooper minimum in argon as an example [18]. We then consider the measurement of recollision in a diatomic molecule [8, 19], which exhibits a π -phase jump in its transition moment due to two-centre interference. We will demonstrate that *in situ* measurement is generally sensitive to the transition moment phase, but insensitive to phase shifts arising from ionic structure.

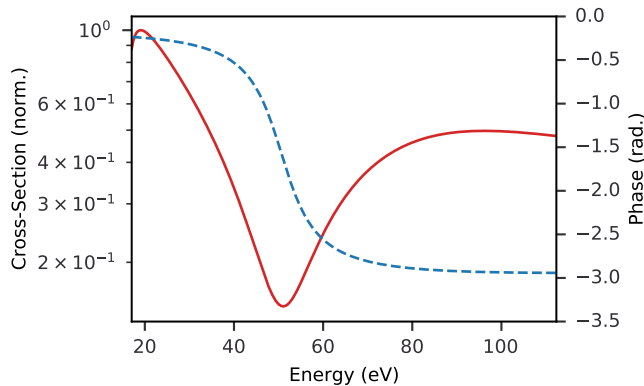


FIG. 1. The recombination cross-section (solid red) and phase (dashed blue) for the model argon atom are plotted on the left and right axes, respectively. A spectral minimum and π -phase shift occur near 52 eV.

For consistency, all our results are calculated using a sinusoidal driving field with wavelength 1.8 m and peak intensity of 1×10^{14} W/cm² and a perturbing co-polarized second-harmonic field with a relative intensity 10^{-4} .

A. Cooper Minimum in Argon

We consider an atomic system of ionization potential 15.8 eV with a transition moment cross-section and phase as depicted in Fig. 1. A spectral minimum and π -phase shift are observed near 52 eV. We choose this model, as it provides a simple description of the transition moment phase in argon including both s - and d -wave continuum channels [7]. We incorporate the transition moment phase $\Phi(k)$ at momentum k into the saddle-point analysis of the SFA by using the following modified saddle-point equations to find the dipole moment in the time domain:

$$0 = \int_{t_b}^{t_r} P(\tau) d\tau - \Phi'(P(t_r)) + \Phi'(P(t_b)), \quad (15)$$

$$0 = \frac{P^2(t_b)}{2} + I_p + E(t_b)\Phi'(P(t_b)), \quad (16)$$

We numerically solve Eqs. (15) and (16) in the time domain for the saddle-point solutions with the transition moment phase in Fig. 1. Figure 2 (a) depicts the trajectory excursion time as a function of the emitted photon energy from the system including the transition moment phase (solid red) and a reference equivalent system without the transition moment phase (dashed blue). The excursion time for the system with the transition moment phase shift deviates from the reference system around 52 eV due to the transition moment phase shift. This difference is depicted in Fig. 2 (b) along the left axis (solid red) and is largest (-145 as) near 50 eV.

Within the modified saddle-point equations, the gradient of the transition moment phase acts equivalently to a

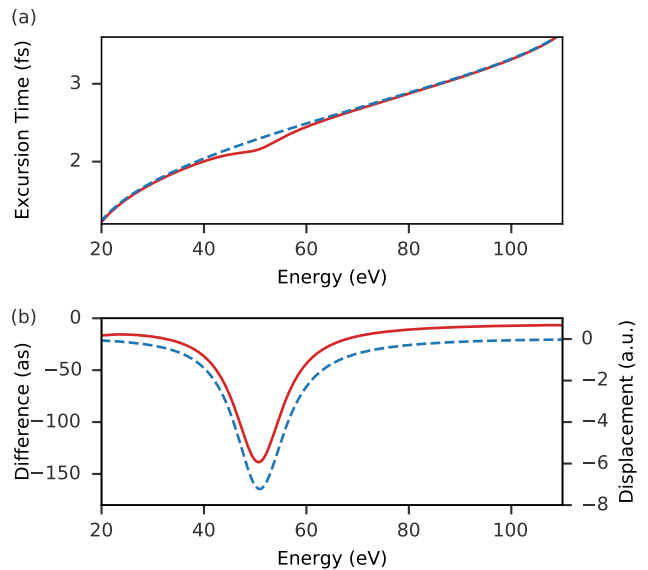


FIG. 2. (a) The short-trajectory excursion times as a function of emitted photon energy calculated with (solid red) and without (dashed blue) the transition-moment phase from Fig. 1 in Eqs. (15-16). (b) The difference in excursion time between the systems with and without the transition moment phase from the excursion times presented in (a) (solid red) are plotted on the left axis. The difference in the positions of ionization and recombination for the trajectories leading to photon emission at a given energy (dashed blue) are plotted on the right axis. The sinusoidal driving field intensity and wavelength are 1×10^{14} W/cm⁻².

spatial offset. The return condition in Eq. (15) is offset by the difference in the transition moment phase at the times of ionization and recombination. In Eq. (16), the condition for energy conservation during the ionization step, is shifted in energy analogously to a dipole interaction between the driving electric field and the transition moment phase gradient. Thus, we expect the relative positions of ionization and recombination to depend on the gradient of the transition moment phase.

Fig. 2(b) shows the difference between the positions of ionization and recombination, Δx , along the right axis (dashed blue). The structure of Δx reflects the structure of the change in excursion time. In argon, the Cooper minimum results from the nodal structure of the ground state wavefunction [18], wherein the radial ground state wavefunction exhibits a tightly-bound inner lobe and a larger outer lobe with a radial extent of ~ 10 a.u. Below the spectral minimum, dipole emission from the outer lobe dominates dipole emission. At the spectral minimum, the dipole emission from these lobes cancels. Above the spectral minimum, the lobe which dominates dipole emission changes, resulting in a shift in the position of photon emission. Thus, we interpret the variation in Fig. 2 (b) as a consequence of the structure of the ground state wavefunction.

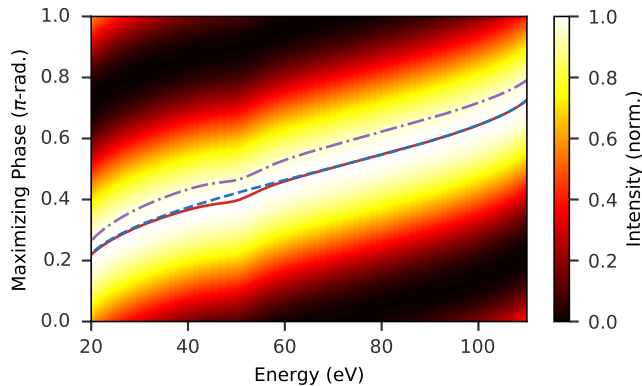


FIG. 3. The spectrogram showing variation of the even-harmonic intensity in an *in situ* measurement of the model argon atom with respect to the relative phase between the driving and perturbing fields. The overlaid solid red and dashed blue lines show the maximizing phase for the model argon and reference atoms, respectively. The overlaid purple dash-dotted line depicts the scaled excursion time as shown in Fig. 2. The driving field intensity and wavelength are 1×10^{14} W/cm $^{-2}$.

We are now ready to consider an *in situ* measurement. We use Eqs. (8) and (11) to calculate the phase $\theta(k, t_b, t_r)$ which maximizes the even-harmonic signal and Eq. (14) to calculate the variation of the even-harmonic intensity with the relative phase between the driving and perturbing fields. We perform the same calculation for an equivalent system without a transition moment phase to use as a reference.

The resultant spectrogram depicting the normalized variation of the even-harmonic intensity with the relative phase between the driving and perturbing fields is shown in Fig. 3. The overlaid solid red line depicts the maximizing phase $\theta(k, t_b, t_r)$ calculated from the model argon atom while the dashed blue line shows the same result for the reference atom. A clear deviation from the reference around 52 eV is observed in the result that includes the transition moment phase. Above and below the resonance, the two results agree. The trajectory excursion time from our model argon atom (dot-dash purple) agrees with the maximizing phase, indicating that *in situ* measurement is sensitive to the transition moment phase. This result agrees with recent experimental and theoretical work [14] reporting the *in situ* measurement of photorecombination time delays around the Cooper minimum in argon.

As mentioned previously, however, it is well-accepted within the attosecond science community that *in situ* measurement is incapable of measuring the transition moment phase [8]. It is argued that the perturbing field does not significantly affect the transition moment enough to have a measurable effect. However, as demonstrated in Section IA and Fig. 2, the perturbing field doesn't need to affect the transition moment. Attosec-

ond pulse generation occurs when the continuum electron wave packet overlaps with the ground state, resulting in an oscillating dipole which returns the system to its initial state. The components of the recollision electron wave packet which dominate dipole emission are determined through phase-matching conditions dictated by the strong driving field and atomic or molecular system. In systems with a real, or slowly varying, transition moment, the phase-matching conditions are determined by the strong driving field and result in the well-known attochirp.

In systems with a rapidly varying transition moment phase, however, the variation of the transition moment phase can be comparable to that of the semi-classical action. In such cases, the transition moment phase must be taken into account in the SFA saddle-point analysis, as in Section IA. The transition moment phase then modifies the phase matching conditions and, thus, which recollision trajectories dominate dipole emission. These trajectories are measurable and this measurement does not require the perturbing field to affect the transition moment.

B. Ionic Structure

We now address the apparent discrepancy between the recent experimental and theoretical study of an *in situ* measurement in argon [14] and the study which demonstrated attosecond *in situ* measurement is insensitive to the transition moment phase associated with two-centre interference in diatomic molecular systems [8]. The two-center study compared attosecond *in situ* measurement with a conventional photoionization-based attosecond measurement technique [13] and found that, while the conventional measurement is sensitive to the transition moment phase, the effect of the phase shift was completely absent from the *in situ* measurement. Here, we show that our analysis is consistent with that study. The insensitivity of *in situ* measurement to two-centre interference is a characteristic of phase shifts arising from ionic structure.

There are several methods for calculating recollision processes in diatomic molecules using the SFA. We use the formalism presented in [23], due to the agreement of the dipole phase with numerical time-dependent Schrödinger equation simulations. For simplicity, we consider a one-dimensional diatomic molecule with atomic centres located at $x = \pm R/2$, where R is the internuclear separation. We label the atomic centres of ionization and recombination as $\alpha, \beta = 1, 2$, respectively, such that the positions of ionization and recombination are $(-1)^\gamma R/2$ with $\gamma = \alpha, \beta$. Accordingly, we label the parameters for each trajectory with the subscript $\alpha\beta$. Our analysis can be easily extended to more complex systems.

We describe the ground state $\psi(x)$ using a linear combination of atomic orbitals (LCAO) centred at each atomic centre. Recombination and ionization from atom

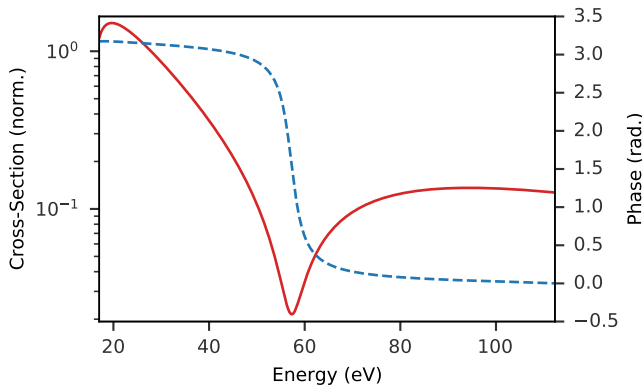


FIG. 4. The recombination cross-section and phase for a one-dimensional diatomic molecule with an internuclear separation of 1.8 a.u. and ionization potential of 15.8 eV calculated using eqs. (21-23), the first-order approximation given in [23], and a sinusoidal driving field of wavelength 1.8 m and peak intensity 1×10^{14} W/cm².

α at momentum k and time t are described by the following matrix elements:

$$d_{rec}(k) = \mathcal{R}(k) \left(e^{ikR/2} + e^{-ikR/2} \right), \quad (17)$$

$$d_{ion}(k, t) = \mathcal{J}_1(k, t)e^{ikR/2} + \mathcal{J}_2(k, t)e^{-ikR/2}, \quad (18)$$

where $\mathcal{R}(k)$ and $\mathcal{J}_\alpha(k, t)$ denote the recombination and ionization matrix elements for the atomic orbital which makes up the ground state. With these, the recollision dipole spectrum is represented as the sum of four terms, corresponding to each $\alpha\beta$ trajectory:

$$\begin{aligned} \tilde{D}(\Omega) = & \sum_{\alpha, \beta=1}^2 \int dk \int_{-\infty}^{\infty} dt_r \int_{-\infty}^{t_r} dt_b \mathcal{R}(P(t_r)) \mathcal{J}_\alpha(P(t_b), t_b) \\ & \times e^{-i[S(k, t_b, t_r) - \Omega t_r + \Phi_\alpha(P(t_b)) - \Phi_\beta(P(t_r))]}, \end{aligned} \quad (19)$$

where

$$\Phi_\gamma(k) = (-1)^\gamma k \frac{R}{2} \quad (20)$$

acts as an effective transition moment phase for the $\alpha\beta$ trajectory. From Eq. (20), the gradient of the transition moment phase $\Phi'_\gamma(k) = (-1)^\gamma R/2$ is a constant.

The changes to the saddle-point solutions from a simple atomic system due to the transition moment phase in Eq. (20) are small. As in [23], we find the first-order Taylor expansion of the saddle-point equations in the frequency domain to first-order with respect to R using Eq. (20). We perform this expansion about the saddle-point solutions for a system without a transition moment phase, \bar{k} , \bar{t}_b , and \bar{t}_r , which we label as the zeroth-order

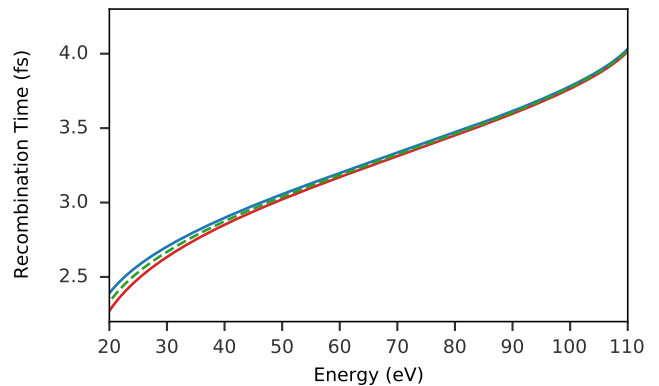


FIG. 5. The recombination times for trajectories recombining to the left (red) and right (blue) atomic centres in a diatomic molecule of internuclear separation $R = 1.8$ a.u. and ionization potential 15.8 eV are shown. The recombination times in a reference atom with an equivalent ionization potential is shown by the dashed green line. A sinusoidal driving field of wavelength 1.8 and peak intensity 1×10^{14} W/cm² is used.

solutions. This results in the following corrections to the saddle-point solutions from the zeroth-order solution for each $\alpha\beta$ trajectory [23]:

$$\Delta k_{\alpha\beta}^{(1)} = 0, \quad (21)$$

$$\Delta t_{b,\alpha}^{(1)} = \frac{(-1)^\alpha R}{2(\bar{k} + A(\bar{t}_b))}, \quad (22)$$

$$\Delta t_{r,\beta}^{(1)} = \frac{(-1)^\beta R}{2(\bar{k} + A(\bar{t}_r))}. \quad (23)$$

As shown in [23], the dipole moment in Eq. (19) can be expanded to first-order in R using these saddle-point corrections. The first-order recombination transition moment cross-section and phase calculated with this model are shown in Fig. 4. Although it appears like the transition moment depicted in Fig. 1 for the model argon atom, the origin of the spectral minimum in each case differs. While the Cooper minimum is a result of the structure of the ground state wavefunction, the spectral minimum here results from the interference of the four possible $\alpha\beta$ trajectories.

From Eqs. (21-23), it is apparent that the individual trajectories do not reflect the spectral structure of the transition moment phase. This is demonstrated in Fig. 5, which shows the recombination times for trajectories with $\beta = 1, 2$ (red and blue solid lines, respectively) and the recombination time for the reference atomic system (dashed green). The correction to the recombination time corresponds to the time required for an electron of kinetic momentum $P(\bar{t}_r)$ to travel a distance of $(-1)^\beta R/2$ and varies adiabatically with the electron kinetic energy.

We now consider an *in situ* measurement in a two-centre system. Since $|\Delta t_{r,\beta}^{(1)}|/\bar{t}_r \ll 1$, we expand Eq. (8) to first-order in $\Delta t_{r,\beta}^{(1)}$ for each $\alpha\beta$ trajectory. A similar

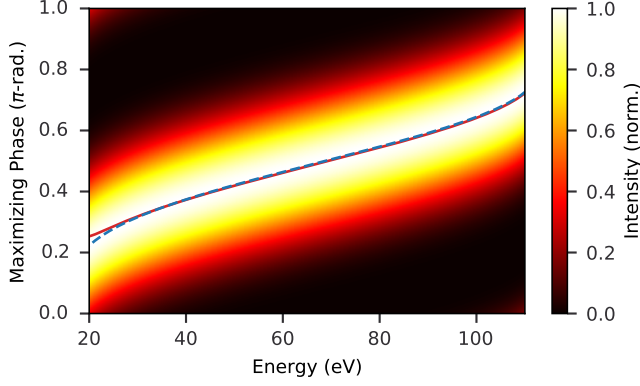


FIG. 6. The spectrogram showing the variation of the even-harmonic intensity in an *in situ* measurement in the two-centre system with respect to the relative phase between the driving and perturbing fields. The overlaid solid red and dashed blue lines show the maximizing phase for the diatomic molecule and reference atom, respectively. The driving field intensity and wavelength are 1×10^{14} W/cm $^{-2}$.

analysis can be done accounting for the correction to the ionization time, but we omit it for brevity. Given that the recollision phase is predominantly shaped by continuum propagation and recombination, this omission does not affect our results or conclusions. To first-order in $\Delta t_{r,\beta}^{(1)}$, the perturbation-induced phase shift for trajectories recombining to atomic centre β can be approximated as follows:

$$\begin{aligned} \sigma_{\beta}(k, t_b, t_r, \phi) &\approx \sigma_0(\bar{k}, \bar{t}_b, \bar{t}_r, \phi) - A_p(\bar{t}_r, \phi) \Phi'_{\beta}(P(\bar{t}_r)) \\ &+ \left(E_p(\bar{t}_r, \phi) \Phi'(P(\bar{t}_r)) + \frac{\partial \sigma_0}{\partial t_r} \Big|_{\bar{k}, \bar{t}_b, \bar{t}_r} \right. \\ &\quad \left. + E(\bar{t}_r) A_p(\bar{t}_r, \phi) \Phi''_{\beta}(P(\bar{t}_r)) \right) \Delta t_{r,\beta}^{(1)}, \end{aligned} \quad (24)$$

where we have solely retained terms which include the perturbing field. Within this first-order approximation, the influence of the perturbing field on the transition moment exactly cancels the change in $\sigma_0(k, t_b, t_r, \phi)$ due to $\Delta t_{r,\beta}^{(1)}$, since

$$\frac{\partial \sigma_0}{\partial t_r} \Delta t_{r,\beta}^{(1)} = A_p(\bar{t}_r, \phi) \Phi'_{\beta}(P(\bar{t}_r)). \quad (25)$$

Further, the phase $\Phi_{\beta}(k)$ varies linearly with respect to momentum and, therefore, $\Phi'_{\beta}(k) = 0$. The total perturbation-induced phase shift is then given as follows:

$$\sigma_{\beta}(k, t_b, t_r, \phi) = \sigma_0(\bar{k}, \bar{t}_b, \bar{t}_r, \phi) + \frac{E_p(\bar{t}_r, \phi)}{\bar{k} + A(\bar{t}_r)} R^2. \quad (26)$$

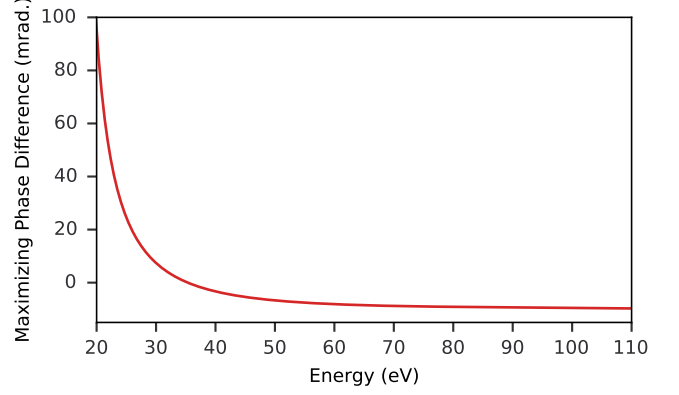


FIG. 7. The difference in the maximizing phase between the diatomic molecule and reference atomic systems from the simulated *in situ* measurement in Fig. 6.

The effective perturbation-induced phase shift is equal to the sum of that in a system without a transition moment phase and a term proportional to the square of the distance of the displaced recombination atomic centre to the origin. Thus, all trajectories exhibit the same perturbation-induced phase shift. Further, the change in the perturbation-induced phase shift is small, since $\omega_0 \ll 1$. Therefore, the results of an *in situ* measurement in a two-centre system and reference atomic system will exhibit negligible differences. This is in contrast to the study of the Cooper minimum in argon, wherein the transition moment phase is not a linear function of momentum and the large variation of the phase shift within a single recollision trajectory necessitates higher-order descriptions of the measurement.

This is confirmed in Fig. 6, which depicts a spectrogram of the variation of the even-harmonic intensity with the relative phase between the driving and perturbing fields. The overlaid solid red and dashed blue lines depict the maximizing phase for the two-centre and an equivalent reference atomic system. The results for the diatomic molecule and reference atomic system are nearly identical, except at low energies, and the structure of the phase jump in Fig. 4 is completely absent. The difference in the maximizing phase for the two-centre and reference atomic systems is shown in Fig. 7. Like the change in recombination time due to molecular structure, the difference in maximizing phase between the two-centre and reference atom is largest at low energies and decreases monotonically with energy.

This result implies the nature of the transition moment phase is critical in determining the sensitivity of *in situ* measurement to recombination dynamics. We expect that we can use differences between a conventional photoionization-based streaking experiment and an *in situ* measurement to isolate spectral features of attosecond pulses due to ionic and electronic structure and dynamics.

III. CONCLUSION

The sensitivity of attosecond *in situ* measurement to transition moment phase shifts is explained by how the transition moment phase affects recollision trajectories. If the transition moment is real or its phase varies sufficiently slowly, then its effect on recollision trajectories is negligible and the semi-classical action dictates the phase-matching conditions. If, however, the transition moment is complex and rapidly varying, its phase can be as important in determining the stationary points as the semi-classical action. Since the ground state wavefunction is negligibly varied, phase matching favours components of the recollision wave packet with a spectral phase that complements the transition moment phase.

Our results demonstrate that the nature of the transition moment phase determines its effect on recollision trajectories and, thereby, the sensitivity of *in situ* measurement to such phase shifts. In particular, *in situ* measurement is sensitive to the transition moment phase, but insensitive to phase shifts due to two-centre interference. Thus, we explain the apparent discrepancy between recent experiments reporting photorecombination time delay measurements using *in situ* techniques in argon [12] and studies which showed these techniques are insensitive to the phase jump from two-centre interference. Although we investigated recollision in a diatomic molecule, our results are easily extended to more complex molecular systems.

The all-optical measurements of photorecombination time delays offers a new direction for attosecond measurement without obfuscation from ionic structural effects and can be performed in any laboratory capable of generating high harmonic radiation. Such measurements can be used to characterize multielectron interaction [24–26], electronic structure [14, 27], and strong-field-driven electron dynamics.

Further, the relationship between photorecombination time delays and electronic structure suggests a form of tomography [28, 29], wherein electronic structure is inferred from all-optical measurements. Finally, by combining *in situ* measurement with methods such as the attosecond streak camera or reconstruction of attosecond bursts by two-photon transitions (RABBITT), ionic and electronic effects on the phase of attosecond and high harmonic pulses can be isolated.

ACKNOWLEDGMENTS

Acknowledgements: This research was supported by the United States Air Force Office of Scientific Research (award #: FA9550-16-1-0109) with contributions from the Canada Foundation for Innovation, the Canada Research Chairs program, Canada’s Natural Sciences and Engineering Research Council and the National Research Council of Canada.

-
- [1] N. Dudovich, O. Smirnova, J. Levesque, Y. Mairesse, M. Y. Ivanov, D. M. Villeneuve, and P. B. Corkum, Measuring and controlling the birth of attosecond xuv pulses, *Nature Physics* **2**, 781 (2006).
 - [2] K. T. Kim, D. M. Villeneuve, and P. B. Corkum, Manipulating quantum paths for novel attosecond measurement methods, *Nature Photonics* **8**, 187 (2014).
 - [3] M. Lewenstein, P. Balcou, M. Y. Ivanov, A. L’Huillier, and P. B. Corkum, Theory of high-harmonic generation by low-frequency laser fields, *Phys. Rev. A* **49**, 2117 (1994).
 - [4] P. B. Corkum, Plasma perspective on strong field multiphoton ionization, *Phys. Rev. Lett.* **71**, 1994 (1993).
 - [5] K. Varjú II, Y. Mairesse, B. Carré, M. B. Gaarde, P. Johnsson, S. Kazamias, R. López-Martens, J. Mauritsson, K. J. Schafer, P. Balcou, A. L’Huillier, and P. Salières, Frequency chirp of harmonic and attosecond pulses, *Journal of Modern Optics* **52**, 379 (2005).
 - [6] M. Lewenstein, P. Salières, and A. L’Huillier, Phase of the atomic polarization in high-order harmonic generation, *Phys. Rev. A* **52**, 4747 (1995).
 - [7] S. B. Schoun, R. Chirla, J. Wheeler, C. Roedig, P. Agostini, L. F. DiMauro, K. J. Schafer, and M. B. Gaarde, Attosecond pulse shaping around a cooper minimum, *Phys. Rev. Lett.* **112**, 153001 (2014).
 - [8] M. Spanner, J. B. Bertrand, and D. M. Villeneuve, *In situ* attosecond pulse characterization techniques to measure the electromagnetic phase, *Phys. Rev. A* **94**, 023825 (2016).
 - [9] A. D. Shiner, B. E. Schmidt, C. Trallero-Herrero, H. J. Wörner, S. Patchkovskii, P. B. Corkum, J.-C. Kieffer, F. Légaré, and D. M. Villeneuve, Probing collective multi-electron dynamics in xenon with high-harmonic spectroscopy, *Nature Physics* **7**, 464 (2011).
 - [10] G. Orenstein, O. Pedatzur, A. J. Uzan, B. D. Bruner, Y. Mairesse, and N. Dudovich, Isolating strong-field dynamics in molecular systems, *Phys. Rev. A* **95**, 051401(R) (2017).
 - [11] A.-T. Le, T. Morishita, and C. D. Lin, Extraction of the species-dependent dipole amplitude and phase from high-order harmonic spectra in rare-gas atoms, *Phys. Rev. A* **78**, 023814 (2008).
 - [12] A.-T. Le, R. R. Lucchese, S. Tonzani, T. Morishita, and C. D. Lin, Quantitative rescattering theory for high-order harmonic generation from molecules, *Phys. Rev. A* **80**, 013401 (2009).
 - [13] P. M. Paul, E. S. Toma, P. Breger, G. Mullot, F. Augé, P. Balcou, H. G. Muller, and P. Agostini, Observation of a train of attosecond pulses from high harmonic generation, *Science* **292**, 1689 (2001).
 - [14] C. Zhang, G. G. Brown, D. H. Ko, and P. B. Corkum, Optical measurement of photorecombination time delays (2021), arXiv:2104.00844 [physics.atom-ph].
 - [15] J. Itatani, F. Quéré, G. L. Yudin, M. Y. Ivanov,

- F. Krausz, and P. B. Corkum, Attosecond streak camera, *Phys. Rev. Lett.* **88**, 173903 (2002).
- [16] G. Vampa, C. R. McDonald, G. Orlando, P. B. Corkum, and T. Brabec, Semiclassical analysis of high harmonic generation in bulk crystals, *Phys. Rev. B* **91**, 064302 (2015).
- [17] T. T. Luu, Z. Yin, A. Jain, T. Gaumnitz, Y. Pertot, J. Ma, and H. J. Wörner, Extreme-ultraviolet high-harmonic generation in liquids, *Nature Communications* **9**, 3723 (2018).
- [18] J. W. Cooper, Photoionization from outer atomic subshells. a model study, *Phys. Rev.* **128**, 681 (1962).
- [19] C. Vozzi, F. Calegari, E. Benedetti, J.-P. Caumes, G. Sansone, S. Stagira, M. Nisoli, R. Torres, E. Heesel, N. Kajumba, J. P. Marangos, C. Altucci, and R. Velotta, Controlling two-center interference in molecular high harmonic generation, *Phys. Rev. Lett.* **95**, 153902 (2005).
- [20] A. Nayak, M. Dumergue, S. Khn, S. Mondal, T. Csizmadia, N. Harshitha, M. Fle, M. Upadhyay Kahaly, B. Farkas, B. Major, V. Szasz-Bogr, P. Fldi, S. Majorosi, N. Tsatrafyllis, E. Skantzakis, L. Neorii, M. Shirozhan, G. Vampa, K. Varj, P. Tzallas, G. Sansone, D. Charalambidis, and S. Kahaly, Saddle point approaches in strong field physics and generation of attosecond pulses, *Physics Reports* **833**, 1 (2019), saddle point approaches in strong field physics and generation of attosecond pulses.
- [21] K. T. Kim, C. Zhang, A. D. Shiner, S. E. Kirkwood, E. Frumker, G. Gariepy, A. Naumov, D. M. Villeneuve, and P. B. Corkum, Manipulation of quantum paths for space-time characterization of attosecond pulses, *Nature Physics* **9**, 159 (2013).
- [22] D. H. Ko, G. G. Brown, C. Zhang, and P. B. Corkum, Near-field imaging of dipole emission modulated by an optical grating (2020), arXiv:2010.05017 [physics.atom-ph].
- [23] M. Labeye, F. m. c. Risoud, C. Lévêque, J. Caillat, A. Maquet, T. Shaaran, P. Salières, and R. Taïeb, Dynamical distortions of structural signatures in molecular high-order harmonic spectroscopy, *Phys. Rev. A* **99**, 013412 (2019).
- [24] G. G. Brown, D. H. Ko, C. Zhang, and P. B. Corkum, Characterizing fano resonances during recollision (2020), arXiv:2010.04834 [physics.atom-ph].
- [25] S. Pabst and R. Santra, Strong-field many-body physics and the giant enhancement in the high-harmonic spectrum of xenon, *Phys. Rev. Lett.* **111**, 233005 (2013).
- [26] G. G. Brown, D. H. Ko, C. Zhang, and P. B. Corkum, Characterizing multielectron dynamics during recollision (2020), arXiv:2010.06165 [physics.atom-ph].
- [27] S. L. Molodtsov, S. V. Halilov, V. D. P. Servodio, W. Schneider, S. Danzenbächer, J. J. Hinarejos, M. Richter, and C. Laubschat, Cooper minima in the photoemission spectra of solids, *Phys. Rev. Lett.* **85**, 4184 (2000).
- [28] J. Itatani, J. Levesque, D. Zeidler, H. Niikura, H. Pépin, J. C. Kieffer, P. B. Corkum, and D. M. Villeneuve, Tomographic imaging of molecular orbitals, *Nature* **432**, 867 (2004).
- [29] J. B. Bertrand, H. J. Wörner, P. Salières, D. M. Villeneuve, and P. B. Corkum, Linked attosecond phase interferometry for molecular frame measurements, *Nature Physics* **9**, 174 (2013).